# Extreme ultraviolet interferometry measurements with high-order harmonics

**D. Descamps, C. Lyngå, J. Norin, A. L'Huillier, and C.-G. Wahlström**

*Department of Physics, Lund Institute of Technology, P.O. Box 118, S-221 00 Lund, Sweden*

**J.-F. Hergott, H. Merdji, and P. Salières**

*Service des Photons, Atomes, et Molécules, Centre d'Etudes de Saclay, 91191 Gif-sue-Yvette, France*

**M. Bellini**

*European Laboratory for Non Linear Spectroscopy, Largo E. Fermi, 2, I-50125 Florence, Italy*

**T. W. Hänsch**

*Max-Planck-Institut für Quantenoptik, P.O. Box 1513, D-85740 Garching, Germany*

Received August 10, 1999

We demonstrate that high-order harmonics generated by short, intense laser pulses in gases provide an interesting radiation source for extreme ultraviolet interferometry, since they are tunable, coherent, of short pulse duration, and simple to manipulate. Harmonics from the 9th to the 15th are used to measure the thickness of an aluminum layer. The 11th harmonic is used to determine the spatial distribution of the electron density of a plasma produced by a 300-ps laser. Electronic densities higher than $2-10^{20}$ electrons/cm$^3$ are measured. © 2000 Optical Society of America

*OCIS codes:* 190.0190, 190.4160, 190.7110, 120.3180, 140.7240, 350.4500.

High-order harmonic generation in gases has been studied extensively during the past few years, motivated by the potential of this extreme ultraviolet (XUV) radiation to become a useful source for applications.[1–4] Much effort has been devoted to improving the harmonic-generation conversion efficiency[5–7] as well as characterizing the radiation properties spatially[8,9] and temporally.[10,11] Recently we showed[8,9] that two spatially separated sources of high-harmonic radiation created by the same laser pulse are phase locked[15] and interfere when they are superposed in the far field. This interesting property was used to investigate the temporal coherence of high-order harmonic emission.[13] Our aim in this Letter is to show that phase locking also allows us to perform interferometry in the XUV range to probe thin solid films and dense plasmas.

Interferometry has been demonstrated in the soft-x-ray wavelength range by use of x-ray lasers.[14,15] High-order harmonic generation adds to the technique the major improvements of tunability, ultrashort (subpicosecond) pulse duration, compactness, and simplicity. For some experiments, it is very useful to adjust the wavelength far from an absorption line or band. The spectrum of the harmonic source allows us to obtain interference patterns at different wavelengths corresponding to odd harmonics of the fundamental radiation. High-order harmonic sources can emit during a few tens of femtoseconds. This property offers the unique possibility of studying very fast mechanisms that occur, for example, in ultrashort laser–plasma experiments. Finally, the possibility of creating two phase-locked independent harmonic sources allows us to work with a simple optical setup in which splitting and alignment are done with light beams in the near infrared and not in the XUV.

In this Letter we report what is to our knowledge the first interferometric measurements in the XUV by use of high-order harmonics generated in a gas jet as a source of coherent radiation. The experimental setup is quite similar to that used in previous harmonic temporal coherence studies.[13] We use a terawatt Ti:sapphire laser, operating at 10 Hz and delivering 200-mJ 110-fs pulses in a 9-nm bandwidth centered around 790 nm. The infrared laser pulse is split into two identical pulses in a setup resembling a Michelson interferometer (Fig. 1). In one arm, a mirror is slightly tilted so that focusing of the laser beams results in two spatially separated foci. At the output of the setup, we reduce the aperture of the beam from 25 to 11 mm with an iris located just before the 500-mm focal-length lens that focuses the beams into a pulsed krypton gas jet. The experiment is performed with energy of typically 0.5 mJ in each infrared pulse after the aperture, corresponding to a total energy of 6.5 mJ before the first beam splitter. In these conditions, the peak intensity in each focus is estimated to a few times $10^{14}$ W/cm$^2$. A normal-incidence spherical grating (1200 lines/mm, $f = 500$ mm) is used to select, with the help of a slit, a given harmonic order and to image, with a magnification of 1, the gas-jet plane. From the image plane, the two harmonic beams diverge and overlap in the far field, resulting in an interference pattern. This pattern is observed with microchannel plates (MCP's) coupled to a phosphor screen and captured with a 16-bit CCD camera through a camera objective. The distance between the image plane and the MCP is fixed at 0.9 m.

The far-field fringe pattern can be observed with single-shot acquisition and exhibits good contrast, better than 30% over a large part of the harmonic beam. Using the knife-edge technique in the image focal

0146-9592/00/020135-03$15.00/0 

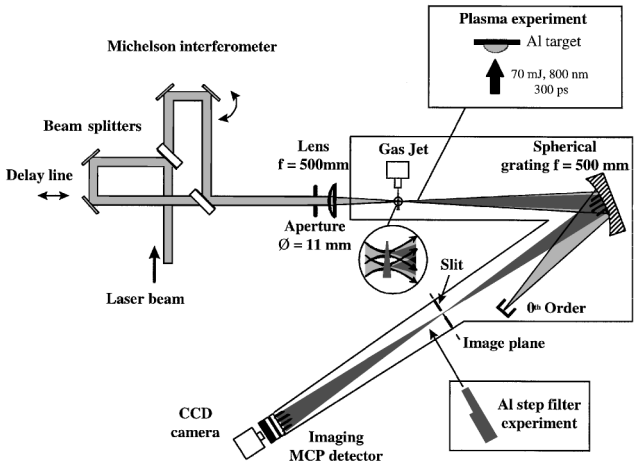


Fig. 1. Experimental setup.

plane, we find a 130-$\mu$m separation between the two images of harmonic sources, as is confirmed by the fringe spacing, and measure the diameter of each of the two foci of the 13th harmonic to be roughly 25 $\mu$m (FWHM). The divergence of the harmonic beams is deduced from the spot size on the MCP detector and found to be equal to approximately 4 mrad.

In the first part of the experiment, we probe a free-standing aluminum step filter, using harmonics of orders 9 to 15 (14–24 eV). Aluminum is chosen for its relatively good transmission in the XUV range and because its refractive index is quite different from unity in the spectral region under consideration,[16] allowing us to obtain a visible fringe shift with a relatively small thickness. The filter is composed of a 100-nm layer. Upon half of this layer we deposit a second layer to build a step. To study the transition region between the two layers we use one harmonic beam (probe beam) that passes through the center of the filter (containing the step) and another (reference beam) that passes through only the thin uniform layer. The aluminum filter is placed 15 mm after the image plane. This position is such that the two beams are still spatially separated but sufficiently far from the beam waist to ensure that the filter is probed by relatively large beams and that the spatial distribution observed on the MCP can be considered almost a pure projection of the filter. A typical interference pattern obtained with the 13th harmonic is presented in Fig. 2. The top part of the image is the reference fringe pattern, and the bottom part includes the phase effect that is due to the larger thickness of aluminum in the path of one beam. The two parts are clearly separated by a blurred region that corresponds to the step. A fringe shift of $0.38\lambda$ is measured between the two fringe patterns, which gives a value of approximately $72 \pm 8$ nm for the aluminum step size (the aluminum refractive index at 60.8 nm is 0.68). Note that these interferometry measurements are not significantly affected by the presence of thin oxide layers, whereas transmission measurements are strongly perturbed by it. This is so because the refractive index of aluminum oxide is comparable with that of aluminum, whereas its absorption coefficient is 1 order of magnitude higher in this spectral region.[16] Similar interference patterns are obtained for the 9th, 11th, and 15th harmonics, with fringe shifts varying from 0.7 to 0.3, consistent with the variation in refractive index of aluminum.

The aim of the second part of the experiment is to demonstrate that our technique can also be used to probe laser-produced plasmas. It is well known that a dense plasma refracts and absorbs visible light. The availability of many odd harmonics allows us to choose a wavelength for the probe, for a given plasma-density range that is short enough to avoid refraction and absorption but long enough to induce a significant dephasing of the beam when it is propagating through the plasma.

The plasma is generated by irradiation of 50-$\mu$m-thick aluminum foil with a 50-mJ 300-ps 790-nm laser pulse, focused with a 17-cm focal-length lens to an intensity of $\sim 10^{13}$ W/cm$^2$. Unlike in the filter experiment, we place the target directly after the gas jet to reduce as much as possible the influence of the bright plasma self-emission on the measurements. Indeed, both the small detection solid angle and the spectral selection owing to the grating allow us to suppress a large part of the plasma emission. The target, placed 25 mm after the gas jet (see Fig. 1), is parallel to the harmonic propagation axis, and the laser producing the plasma is perpendicular to this axis. At this distance the two harmonic beams are still well separated and have a diameter of $\sim 70$ $\mu$m. The beams are aligned so that only one beam is propagating through the plasma. The delay between the plasma-producing laser pulse and the harmonic pulses at the target is held constant at 1.2 ns.

The optimum probe wavelength for studying this plasma is found to be that of the 11th harmonic. Single-shot interference patterns are presented in Fig. 3, together with the approximate positions of the aluminum target. In Fig. 3(a), the target is not irradiated, and the fringe pattern presents good fringe visibility. Figures 3(b) and 3(c) show results obtained with an irradiated target but with slightly different target–probe distances; the probe beam is closer to the target in Fig. 3(c). Compared with that in Fig. 3(a), the noise level in Figs. 3(b) and 3(c) increases slightly owing to self-emission, and the fringes are tilted. To obtain an estimate of the electron density of the

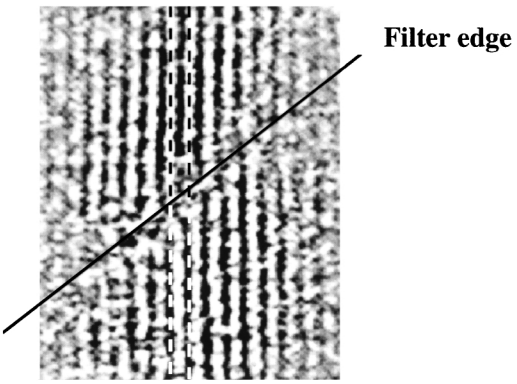


Fig. 2. Interference pattern with the 13th harmonic through an aluminum step filter (two-shot integration). The envelope of the spatial distribution of the harmonic beam is removed by use of a Fourier-transform technique.

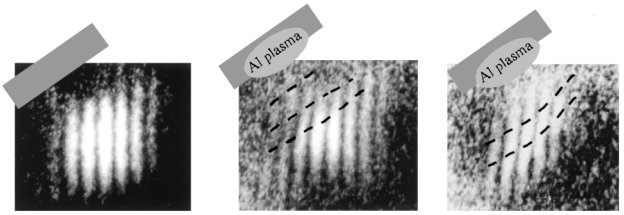


Fig. 3. Single-shot interference patterns obtained with the 11th harmonic (a) without plasma and (b), (c) with plasma. The positions of the plasma are shown in the figure, together with isodensity lines (dashed curves).

plasma, we can approximate the observed fringe shift $N$ (in fringe units) at wavelength $\lambda$:

$$N = \int_0^d \frac{1 - n_{\mathrm{ref}}}{\lambda}\,\mathrm{d}x \approx \frac{\mathrm{d}}{2\lambda}\,\frac{N_e}{N_{\mathrm{cr}}}\,.$$

In Eq. (1), $n_{\mathrm{ref}} = (1 - N_e/N_{\mathrm{cr}})^{1/2}$ is the plasma's refractive index and $d$ is the distance that is traversed by the probe beam through the plasma. We assume that the plasma is uniform along the probe path and that the electron density $N_e$ is much smaller than the critical density $N_{\mathrm{cr}} = 1.1 \times 10^{21}\lambda^{-2}$ ($\lambda$ is in micrometers and $N_{\mathrm{cr}}$ is in inverse cubic centimeters). Refraction effects are neglected. We estimate the distance $d$ experimentally to the order of 0.1 mm by moving the plasma-producing laser beam until the fringe tilt disappears. In Fig. 3(b), only the fringes in the top part of the image are tilted. Those that are far from the target are not perturbed, which allows us to determine the fringe shift that is due to the effect of the plasma and, consequently, the electron density. Isodensity lines corresponding to electron densities of $0.5 \times 10^{20}$, $1 \times 10^{20}$, and $2 \times 10^{20}$ electrons/cm$^3$ (from bottom to top) are indicated by the dashed curves in Fig. 3(b). In Fig. 3(c), the entire probe beam is perturbed by the plasma, which results in a tilt of the whole fringe pattern. This result indicates a quite homogeneous density gradient. Our analysis allows us to give only an upper limit to the electron densities, assuming that the bottom edge of the image is not influenced much by the plasma. Fringe shifts as high as $0.8\lambda$ are observed close to the target surface, indicating densities of at least $2.5 \times 10^{20}$ electrons/cm$^3$. A simulation of the plasma expansion in our experimental conditions has been performed[17] that confirms the absolute values of the electron density as well as the shape of the electron-density gradient obtained from Figs. 3(b) and 3(c).

In conclusion, we have demonstrated the possibility of performing interferometry in the XUV range with higher-order harmonics. We have applied this technique to probe thin solid aluminum films and laser-produced plasmas. The higher-order harmonic source combines a tunable short wavelength and an ultrashort pulse duration, which makes it possible to freeze in time the electron density of an expanding dense plasma. Consequently, this experiment opens new perspectives for the characterization of dense plasmas created in different regimes, from nanosecond to subpicosecond time scales.

The experimental part of this work was carried out at the Lund Laser Centre, Lund, Sweden, with the support of European Community contracts ERBFMGECT950020 and ERBFMBICT983348. D. Deschamps thanks S. Hueller for his plasma simulation. The support of the Swedish Natural Science Research Council and the Göran Gustafsson Foundation for Research in Natural Sciences and Medicine is gratefully acknowledged. D. Descamp's e-mail address is Dominique.Descamps@fysik.lth.se.

## References

1. J. Larsson, E. Mevel, R. Zerne, A. L'Huillier, C.-G. Wahlström, and S. Svanberg, J. Phys. B **28,** L53 (1995).
2. M. Gisselbrecht, D. Descamps, C. Lyngå, A. L'Huillier, C.-G. Wahlström, and M. Meyer, Phys. Rev. Lett. **82,** 4607 (1999).
3. R. Haight and D. Peale, Phys. Rev. Lett. **70,** 3979 (1993).
4. W. Theobald, R. Hässner, C. Wülker, and R. Sauerbrey, Phys. Rev. Lett. **77,** 298 (1996).
5. E. Constant, D. Garzella, P. Breger, E. Mével, C. Dorrer, C. Le Blanc, F. Salin, and P. Agostini, Phys. Rev. Lett. **82,** 1668 (1999).
6. A. Rundquist, C. Durfee III, Z. Chang, C. Herne, S. Backus, M. Murnane, and H. Kapteyn, Science **280,** 1412 (1998).
7. L. Roos, E. Constant, E. Mével, P. Balcou, D. Descamps, M. Gaarde, A. Valette, R. Haroutunian, and A. L'Huillier, Phys. Rev. A **60,** 5010 (1999).
8. P. Salières, T. Ditmire, M. Perry, A. L'Huillier, and M. Lewenstein, J. Phys. B **29,** 4771 (1996).
9. T. Ditmire, E. Grumbell, R. Smith, J. Tisch, D. Meyerhofer, and M. Hutchinson, Phys. Rev. Lett. **77,** 4756 (1996).
10. T. Glover, R. Schoenlein, A. Chin, and C. Shank, Phys. Rev. Lett. **76,** 2468 (1996).
11. A. Bouhal, R. Evans, G. Grillon, A. Mysyrowicz, P. Breger, P. Agostini, R. Constantinescu, H. Muller, and D. von der Linde, J. Opt. Soc. Am. B **14,** 950 (1997).
12. R. Zerne, C. Altucci, M. Bellini, M. Gaarde, T. Hänsch, A. L'Huillier, C. Lyngå, and C.-G. Wahlström, Phys. Rev. Lett. **79,** 1006 (1997).
13. M. Bellini, C. Lyngå, A. Tozzi, M. Gaarde, T. Hänsch, A. L'Huillier, and C.-G. Wahlström, Phys. Rev. Lett. **81,** 297 (1998).
14. L. Da Silva, T. Barbee, R. Cauble, P. Celliers, D. Ciarlo, S. Libby, R. London, D. Matthews, S. Mrowka, J. Moreno, D. Ress, J. Trebes, A. Wan, and F. Weber, Phys. Rev. Lett. **74,** 3991 (1995).
15. F. Albert, D. Joyeux, P. Jaeglé, A. Carillon, J. Chauvineau, G. Jamelot, A. Klisnick, J. Lagron, D. Phalippou, D. Ross, S. Sebban, and P. Zeitoun, Opt. Commun. **142,** 184 (1997).
16. D. Smith, E. Shiles, and A. Inokuti, *Handbook of Optical Constants of Solids*, E. D. Palik, ed. (Academic, San Diego, Calif., 1985), p. 369; F. Gervais, *Handbook of Optical Constants of Solids II*, E. D. Palik, ed. (Academic, San Diego, Calif., 1991), p. 761.
17. S. Hueller, Centre de Physique Théorique, Ecole Polytechnique, 91128 Palaiseau, France (personal communication, July, 1999).